

# An Unusual Solvent Isotope Effect in the Reaction of $W(CO)_5(solv)$ ( $solv = \text{Cyclohexane or Cyclohexane-}d_{12}$ ) with THF

Riki Paur-Afshari, J. Lin, and Richard H. Schultz\*

Department of Chemistry, Bar-Ilan University, Ramat-Gan 52900, Israel

Received October 18, 1999

Time- and temperature-resolved infrared absorption spectroscopy is used to probe the reaction of THF with  $W(CO)_5(solv)$  ( $solv = \text{cyclohexane, cyclohexane-}d_{12}$ ) to form  $W(CO)_5\cdot(THF)$ . In cyclohexane- $d_0$ ,  $\Delta H^\ddagger$  for the reaction is determined to be  $3.6 \pm 0.2 \text{ kcal mol}^{-1}$  ( $15.2 \pm 0.9 \text{ kJ mol}^{-1}$ ) and  $\Delta S^\ddagger = -13.7 \pm 2.5 \text{ eu}$  ( $-57.3 \pm 10.5 \text{ J mol}^{-1} \text{ K}^{-1}$ ). In cyclohexane- $d_{12}$ ,  $\Delta H^\ddagger = 2.4 \pm 0.6 \text{ kcal mol}^{-1}$  ( $10.2 \pm 2.5 \text{ kJ mol}^{-1}$ ) and  $\Delta S^\ddagger = -18.3 \pm 3.5 \text{ eu}$  ( $-76.6 \pm 14.6 \text{ J mol}^{-1} \text{ K}^{-1}$ ). The low activation enthalpy in comparison to the  $(CO)_5W\text{--cyclohexane}$  bond dissociation energy, the negative entropy of activation, and comparison with other spectroscopic experiments involving reactions of  $W(CO)_5(\text{cyclohexane})$  indicate that the reaction proceeds by an associative interchange reaction mechanism. An unusual isotope effect, in which reaction proceeds more slowly in cyclohexane- $d_{12}$  even though  $\Delta H^\ddagger$  is lower, is explained in terms of relative populations of low-frequency vibrations and the relative C–H and C–D bond strengths in the solvent molecule released upon uptake of THF. These experimental results are supported by the results of an ab initio DFT calculation of the structure and vibrational spectrum of  $W(CO)_5(\text{cyclohexane})$ .

## Introduction

The reactions and physical and chemical properties of transition-metal (TM) intermediates have been of considerable interest over the last two decades.<sup>1</sup> A particular area of interest has been trying to understand the properties of coordinatively unsaturated TM intermediates in which a coordination site normally occupied by a strongly bound ligand is "vacant"; it is generally assumed that on the time scale of bimolecular reactions the "vacant" site is actually occupied by a weakly bound solvent molecule. Because such species are so reactive, detecting them and measuring their properties can only be accomplished through sophisticated fast kinetic techniques such as time-resolved infrared spectroscopy (TRIR), time-resolved UV/vis spectroscopy (TR-UV/vis), or photoacoustic calorimetry (PAC). These techniques have succeeded in identifying and characterizing a number of TM intermediates and transient electronic states with lifetimes down to the picosecond time scale.<sup>2–4</sup>

One aspect of the chemistry of such species that has been of particular recent interest has been that of " $\sigma$ -bound" TM–alkane complexes.<sup>5</sup> Such species are known to be intermediates in the photolytic activation of alkane C–H bonds by TM complexes,<sup>6,7</sup> and recently, a low-temperature NMR study provided direct evidence for the existence of a  $\sigma$ -bound  $[CpRe(CO)_2]\text{--cyclopentane}$  complex.<sup>8</sup> In this context, Bergman and Moore and co-workers have performed extensive kinetic studies on the alkane C–H activation reactions of " $Cp^*Rh(CO)$ " generated photolytically in liquid Kr or Xe solution in order to try to elucidate the details of the C–H bond activation process.<sup>9,10</sup> One particularly intriguing result arising from those studies was the observation that the equilibrium between the solvated  $Cp^*Rh(CO)(Kr)$  intermediate and the  $\sigma$ -bound  $Cp^*Rh(CO)(\text{alkane})$  complex appears to favor the alkane complex more strongly upon deuteration of the alkane (i.e., shows an inverse equilibrium isotope effect (EIE)).<sup>9</sup> Because the complex goes on to activate a C–H bond, direct measurement of this effect was not possible. The question of possible isotope

\* To whom all correspondence should be sent. E-mail: schultr@mail.biu.ac.il.

(1) Boese, W.; McFarlane, K.; Lee, B.; Rabor, J.; Ford, P. C. *Coord. Chem. Rev.* **1997**, *159*, 135.

(2) Kelly, J. M.; Long, C.; Bonneau, R. *J. Phys. Chem.* **1983**, *87*, 3344.

(3) (a) Yang, G. K.; Vaida, V.; Peters, K. S. *Polyhedron* **1988**, *7*, 1619.

(b) Morse, J. M., Jr.; Parker, G. H.; Burkey, T. J. *Organometallics* **1989**, *8*, 2471. (c) Braslavsky, S. E.; Heibel, G. E. *Chem. Rev.* **1992**, *92*, 1381.

(d) Hester, D. M.; Sun, J.; Harper, A. W.; Yang, G. K. *J. Am. Chem. Soc.* **1992**, *114*, 5234. (e) Leu, G.-L.; Burkey, T. J. *J. Coord. Chem.* **1995**, *34*, 87.

(4) (a) Welch, J. A.; Peters, K. S.; Vaida, V. *J. Phys. Chem.* **1982**, *86*, 1941. (b) Simon, J.; Peters, K. S. *Chem. Phys. Lett.* **1983**, *98*, 53.

(c) Wang, L.; Zhu, X.; Spears, K. G. *J. Am. Chem. Soc.* **1988**, *110*, 8695.

(d) Lee, M.; Harris, C. B. *J. Am. Chem. Soc.* **1989**, *111*, 8963. (e) Xie, X.; Simon, J. D. *J. Phys. Chem.* **1989**, *93*, 4401. (f) Joly, A. G.; Nelson, K. A. *Chem. Phys.* **1991**, *152*, 69.

(5) Hall, C.; Perutz, R. N. *Chem. Rev.* **1996**, *96*, 3125.

(6) (a) Janowicz, A. H.; Bergman, R. G. *J. Am. Chem. Soc.* **1982**, *104*, 352. (b) Hoyano, J. K.; Graham, W. A. G. *J. Am. Chem. Soc.* **1982**, *104*, 3723. (c) Shilov, A. E.; Shul'pin, G. B. *Chem. Rev.* **1997**, *97*, 2879.

(7) (a) Buchanan, J. M.; Stryker, J. M.; Bergman, R. G. *J. Am. Chem. Soc.* **1986**, *108*, 1537. (b) Periana, R. A.; Bergman, R. G. *J. Am. Chem. Soc.* **1986**, *108*, 7332. (c) Bromberg, S. E.; Yang, H.; Asplund, M. C.; Lian, T.; McNamara, B. K.; Kotz, K. T.; Yeston, J. S.; Wilkens, M.; Frei, H.; Bergman, R. G.; Harris, C. B. *Science* **1997**, *278*, 260.

(8) Geftakis, S.; Ball, G. E. *J. Am. Chem. Soc.* **1998**, *120*, 9953.

(9) (a) Schultz, R. H.; Bengali, A. A.; Tauber, M. J.; Weiller, B. H.; Wasserman, E. P.; Kyle, K. R.; Moore, C. B.; Bergman, R. G. *J. Am. Chem. Soc.* **1994**, *116*, 7369. (b) Bengali, A. A.; Schultz, R. H.; Moore, C. B.; Bergman, R. G. *J. Am. Chem. Soc.* **1994**, *116*, 9585.

(10) (a) Weiller, B. H.; Wasserman, E. P.; Bergman, R. G.; Moore, C. B. *J. Am. Chem. Soc.* **1989**, *111*, 8288. (b) McNamara, B. K.; Yeston, J. S.; Bergman, R. B.; Moore, C. B. *J. Am. Chem. Soc.* **1999**, *121*, 6437.

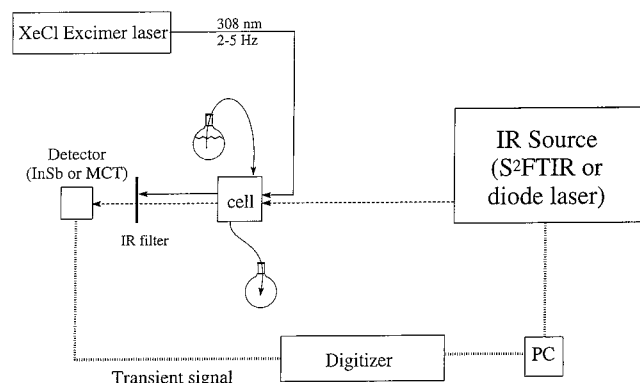
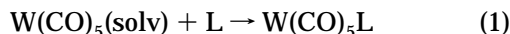


**Figure 1.** Instrumental schematic.

effects in the  $\sigma$ -binding of small molecules (e.g., dihydrogen or alkanes) to transition-metal centers has been of some theoretical interest as well.<sup>11,12</sup>

We wanted to try to see if we could observe a similar effect in a system that does *not* activate the C–H bonds in order to see if a significant isotope effect is a fundamental property of TM–alkane interactions. To this end, we chose to study the temperature and reactant concentration dependences of a reaction of the  $\sigma$ -bound complex of tungsten pentacarbonyl with cyclohexane (CyH) or its perdeuteriated analogue (CyD). In the present study, we obtain activation parameters for the simplest possible reaction of such a species, ligand exchange to form a stable complex, reaction 1.



In these experiments, “solv” = CyH or CyD and “L” = THF.

The primary goal of this experiment was to determine the nature of the isotope effect on the  $\sigma$ -binding of an alkane to a transition-metal fragment by observing what effect deuteration of the alkane has on the course of reaction 1. A second goal was to compare the activation parameters for reaction 1 in CyH and CyD in order to see what insight such measurements could give about the dynamics and mechanism of this ligand substitution reaction itself. Finally, an *ab initio* density-functional theory (DFT) calculation of the structure of the  $W(CO)_5$ –(CyH) complex was performed in order to see what additional insight into the dynamics of reaction 1 we could obtain from a more detailed understanding of the structure of the reactant.

## Experimental Section

**1. General Comments.** The experiments described in this paper were performed on our recently constructed transient infrared (TRIR) spectrometer. An instrumental schematic is shown in Figure 1. Reaction takes place in a temperature-controllable ( $\pm 1^\circ\text{C}$  in the experiments described here), 0.5 mm path length  $\text{CaF}_2$  IR cell (International Crystal Laboratories CryoTherm with model 2405-4761 temperature controller). A reaction solution containing typically  $(2.5\text{--}5) \times 10^{-4} \text{ mol L}^{-1}$   $W(CO)_6$  in CyH or CyD and a large excess of THF undergoes photolysis by the 308 nm pulsed output (ca. 20 ns pulse width, typically 50–80 mJ/pulse at the laser) of a XeCl excimer laser

(Lambda Physik model Compex 102). The photolysis pulse produces the transient  $W(CO)_5(solv)$  complex. Typically, the reaction solution flows through the cell (flow is maintained by a Fluid Metering Systems PiP pipet pump) to ensure that each laser pulse irradiates fresh solution. Reaction progress is monitored by measuring the time-dependent absorption of the IR light emanating from one of two sources described in detail below. Reaction conditions were chosen to keep  $\Delta A_0 < 0.1$  for the intermediate in order to ensure a linear relation between the concentration of the intermediate and the observed absorbance changes. As a preliminary test of the instrument, we performed measurements of the reaction of  $W(CO)_5(\text{CyH})$  with hex-1-ene and obtained rate constants that were within experimental error of those of Dobson and co-workers in their TR-UV/vis study of reaction 1.<sup>16</sup>

**2. Step-Scan FTIR (S²FTIR).** For determination of time-dependent IR spectra, we use an S²FTIR spectrometer<sup>13</sup> (Bruker model Equinox 55 running OPUS 3.0 software) as the IR source. The IR output of the spectrometer exits the instrument, is collimated by a parabolic mirror, passes through the cell, is collected by an elliptical mirror, and impinges on an MCT detector (Kolmar model PV11-1-J2, active area 1 mm², rise time 18 ns) with separate ac and dc preamplifier outputs. For this experiment, signal digitization is done by a 250 MHz PAD 82a fast A/D converter; output of the ac channel of the detector preamplifier is used to monitor the time-dependent signals, and phase correction is done by simultaneous monitoring of the dc output of the detector preamplifier. To maximize the resulting signal-to-noise ratio, preliminary experiments are done to obtain peak dc and ac signals as close as possible to  $\pm 1 \text{ V}$ , the maximum input to the PAD 82a board. Signal maximization of the dc channel is performed by using an oscilloscope to measure the interferogram obtained on a static reaction solution. The source aperture is opened until the detector signal is maximized without clipping; one of a series of home-built high-frequency signal attenuators is then used to bring the signal to approximately  $\pm 0.9 \text{ V}$ . The ac signal is then measured under nominal photolysis conditions and amplified (Stanford Research Systems model SR445 300 MHz amplifier) to bring the peak ac signal as close as possible to 1 V.

S²FTIR spectra are normally obtained at  $4 \text{ cm}^{-1}$  resolution. To minimize the number of data points needed for the interferogram, as well as to protect the detector from stray UV light, IR filters are placed in front of the detector and between the IR source and cell. For these experiments, OCLI model W04944-8 filters (10% cutoffs at approximately 2280 and  $1810 \text{ cm}^{-1}$ ) were used, and spectra were collected over the range  $1760\text{--}2340 \text{ cm}^{-1}$ . Typically, 5–10 laser shots are averaged at each mirror position, and a stabilization delay of 150–200 ms is used at each mirror position prior to photolysis.

**3. Diode Laser Source.** For collection of kinetic data, a diode laser source is used. In this apparatus, a liquid  $\text{N}_2$  cooled

(13) (a) Palmer, R. A.; Manning, C. J.; Rzepiela, J. A.; Widder, J. M.; Chao, J. L. *Appl. Spectrosc.* **1989**, *43*, 193. (b) Uhmman, W.; Becker, A.; Taran, C.; Siebert, F. *Appl. Spectrosc.* **1991**, *45*, 390. (c) Manning, C. J.; Palmer, R. A.; Chao, J. L. *Rev. Sci. Instrum.* **1991**, *62*, 1219. (d) Manning, C. J.; Griffiths, P. R. *Appl. Spectrosc.* **1993**, *47*, 1345. (e) Palmer, R. A.; Chao, J. L.; Dittmar, R. M.; Gregoriou, V. G.; Plunkett, S. E. *Appl. Spectrosc.* **1993**, *47*, 1297. (f) Johnson, T. J.; Simon, A.; Weil, J. M.; Harris, G. W. *Appl. Spectrosc.* **1993**, *47*, 1376. (g) Powell, J. R.; Crocombe, R. A. *Proc. SPIE-Int. Soc. Opt. Eng.* **1993**, *2089*, 244.

(14) Hermann, H.; Grevels, F.-W.; Henne, A.; Schaffner, K. *J. Phys. Chem.* **1982**, *86*, 5151.

(15) Although the code was written independently, the following sources were consulted for development of the algorithms: (a) Natrella, M. G. *Experimental Statistics*; National Bureau of Standards: Washington, D.C., 1963. (b) Bevington, P. R.; Robinson, D. K. *Data Reduction and Error Analysis for the Physical Sciences*, 2nd ed.; McGraw-Hill: New York, 1992. (c) Press, W. H.; Teukolsky, S. A.; Vetterling, W. T.; Flannery, B. P. *Numerical Recipes in C*, 2nd ed.; reprinted with corrections; Cambridge University Press: New York, 1994.

(16) Dobson, G. R.; Asali, K. J.; Cate, C. D.; Cate, C. W. *Inorg. Chem.* **1991**, *30*, 4471.

(11) Bender, B. *J. Am. Chem. Soc.* **1995**, *117*, 11239.

(12) (a) Abu-Hasanayn, F.; Krogh-Jespersen, K.; Goldman, A. S. *J. Am. Chem. Soc.* **1993**, *115*, 8019. (b) Schaller, C. P.; Bonanno, J. B.; Wolczanski, P. *J. Am. Chem. Soc.* **1994**, *116*, 4133.

continuously tunable lead-salt diode laser (Muetek model DH4, range 1830–2050  $\text{cm}^{-1}$ ) is used as a source of CW IR light. The output of the laser is collimated to a 4–5 mm diameter beam, after which it passes through a monochromator (SPEX model 270M, 150 grooves/mm grating blazed at 4  $\mu\text{m}$ , calibrated from successive orders of a He–Ne laser and normally run at  $\sim 1 \text{ cm}^{-1}$  resolution), then through the cell collinear with the UV beam, and on to the detector. For the experiments described here, an InSb detector (Cincinnati Electronics model SDD-32E0-S1-05M, 2  $\text{mm}^2$  active area, rise time 50 ns) was used. The detector output is sent to a digital oscilloscope (LeCroy model 9310A, 100 MS/s) for collection and averaging. Typically, each kinetic trace is the average of the signal following 10–100 laser shots. A background trace is then taken and subtracted from the transient signal, and the combined signal passed via a GPIB interface to a PC for storage.

**4. Reagents.** For the experiments described here,  $\text{W}(\text{CO})_6$  (99%) was obtained from Strem and used without further purification. Cyclohexane was obtained in spectrophotometric or HPLC grade (>99.8% purity) and distilled from Na/benzophenone immediately prior to use. Cyclohexane- $d_{12}$  (99.6% D) was obtained from Aldrich and used without further purification; isotopic purity and freedom from contamination by  $\text{H}_2\text{O}$  were confirmed by  $^1\text{H}$  NMR spectroscopy. THF (99.9%, anhydrous grade, inhibitor-free, used and stored under Ar) was obtained from Aldrich and used without further purification. After preparation, reaction solutions were degassed with Ar and kept under an Ar atmosphere for the duration of the experiment. No evidence for interference from residual water in the solvent<sup>14</sup> or in the THF was observed.

**5. Data Analysis.** For each kinetic run, the pseudo-first-order rate constant  $k_{\text{obs}}$  is determined either by a weighted linear least-squares fit to  $\ln(\Delta A_{\infty} - \Delta A_0)$  or by a nonlinear least-squares single-exponential fit to  $\Delta A$  itself; the two fitting methods yield values for  $k_{\text{obs}}$  for a single kinetic run that do not differ significantly. Reported values for  $k_{\text{obs}}$  normally represent the average of at least two independent data sets. For low concentrations, the reported values include determinations based on both the rate of decay of the intermediate and the rate of growth of the product. Because our diode laser is significantly less powerful at the absorbance peak of the product than it is at that of the intermediate, and because the product peak absorption is less intense than the intermediate peak absorption, we found that at higher rates the S/N ratio for the product growth was not always sufficiently high to produce reliable values for  $k_{\text{obs}}$ ; in these cases, the reported rate was determined from the intermediate decay alone. In all cases, the rate of growth of the product was consistent with the rate of decay of the intermediate. Pseudo-first-order rate constants are reported with  $1\sigma$  uncertainties in the precision. We estimate the absolute uncertainties in  $k_{\text{obs}}$  to be approximately  $\pm 10\%$ , based on uncertainties in the concentration and temperature and on long-term run-to-run reproducibility; these absolute uncertainties are not included in the rate constants reported in Tables S-1 and S-2.

Second-order rate constants and activation parameters were determined by linear least-squares fits to the concentration dependence of  $k_{\text{obs}}$  and are reported with  $1\sigma$  uncertainties. Reported uncertainties for the Eyring activation parameters are 90% confidence limits to least-squares linear fits weighted by the variances of the rate constants. The linear fits were performed using “C” computer programs written in our laboratory;<sup>15</sup> exponential fits were performed with commercially available software.

## Results

**$\text{W}(\text{CO})_5(\text{CyH}) + \text{THF}$ .** Time-dependent  $\text{S}^2\text{FTIR}$  spectra of the reaction of  $\text{W}(\text{CO})_5(\text{CyH})$  with THF (1900–2000  $\text{cm}^{-1}$ ) are shown in Figure 2. At the flash, a bleach corresponding to loss of parent  $\text{W}(\text{CO})_6$  appears, along

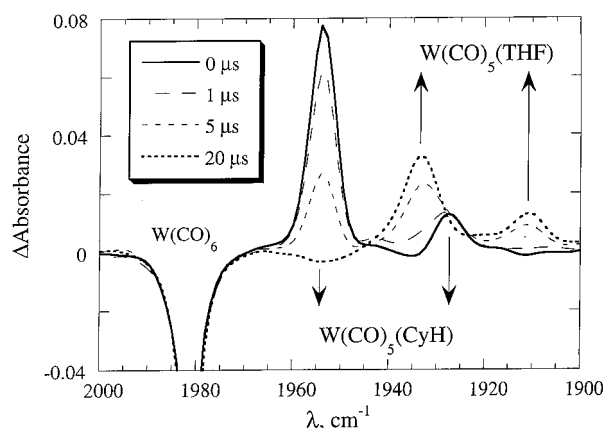


**Figure 2.**  $\text{S}^2\text{FTIR}$  difference spectra (room temperature) for the reaction of  $\text{W}(\text{CO})_5(\text{CyH})$  with  $0.015 \text{ mol L}^{-1}$  THF. Shown are  $\Delta A$  (absorbance change relative to absorbance prior to photolysis) as a function of energy (1900–2000  $\text{cm}^{-1}$ ) at the photolysis flash and at time intervals of 1, 5, and 20  $\mu\text{s}$  following photolysis. The two peaks at 1954 and 1928  $\text{cm}^{-1}$  that decrease with time are attributed to  $\text{W}(\text{CO})_5(\text{CyH})$ ; the two peaks at 1933 and 1912  $\text{cm}^{-1}$  that increase with time are attributed to  $\text{W}(\text{CO})_5(\text{THF})$ ; and the bleach at 1881  $\text{cm}^{-1}$  corresponds to loss of  $\text{W}(\text{CO})_6$ .

with two new peaks at 1954 and 1928  $\text{cm}^{-1}$ , which we assign to the E and  $A_1$  C–O stretches of  $\text{W}(\text{CO})_5(\text{CyH})$ .<sup>14</sup> These two peaks disappear with time, and simultaneously, two new peaks, at 1933 and 1912  $\text{cm}^{-1}$ , corresponding to the E and  $A_1$  C–O stretches of  $\text{W}(\text{CO})_5(\text{THF})$ , grow in with the same time dependence. Symmetry arguments require that there be a third C–O stretch of  $A_1$  symmetry. This very weak peak (on the order of 1–5% of the intensity of the E stretch), not shown in Figure 2, occurs at 2087  $\text{cm}^{-1}$  for  $\text{W}(\text{CO})_5(\text{CyH})$  and at 2074  $\text{cm}^{-1}$  for  $\text{W}(\text{CO})_5(\text{THF})$  in CyH solution.

The diode laser source was used for the actual kinetic measurements. At each temperature and THF concentration, kinetic traces were obtained by setting the diode laser to a frequency corresponding to an absorption of the  $\text{W}(\text{CO})_5(\text{CyH})$  transient and measuring the time-dependent signal at that frequency, and then making the same measurement at a frequency corresponding to an absorbance of the  $\text{W}(\text{CO})_5(\text{THF})$  product. While the  $\text{S}^2\text{FTIR}$  experiment shows that the peak absorbance of the  $\text{W}(\text{CO})_5(\text{CyH})$  transient is at 1954  $\text{cm}^{-1}$ , due to the output characteristics of the diode laser (and possibly to slight uncertainties in the mutual calibrations of the two instruments), we found that the best signal-to-noise ratio was obtained when we set the diode laser to 1955 or 1956  $\text{cm}^{-1}$ . Kinetic measurements made at a variety of frequencies near the product peak showed no dependence of the reaction rate constant on the frequency being probed (i.e., the absorbance line shape is independent of time), however. Typical kinetic traces are shown in Figure 3. Kinetic traces were obtained at five temperatures from 20 to 60  $^\circ\text{C}$  and over a THF concentration range of 0.004–0.24  $\text{mol L}^{-1}$ , and results are shown in Figure 4. The observed pseudo-first-order rate constant is linear with increasing [THF]; linear fits to  $k_{\text{obs}}$  as a function of [THF] are also shown in the figure.

**$\text{W}(\text{CO})_5(\text{CyD}) + \text{THF}$ .** We also measured the kinetics of reaction 1 with solv = CyD over the concentration range [THF] = 0.005–0.1  $\text{mol L}^{-1}$ . Because of the



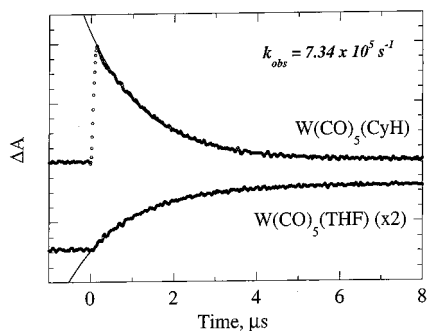


**Figure 3.** Typical diode laser transient traces. Shown are time-dependent absorbances at  $1956\text{ cm}^{-1}$ , due to absorption by  $W(CO)_5(CyH)$ , and at  $1933\text{ cm}^{-1}$  ( $\times 2$ ), due to absorption by  $W(CO)_5(THF)$ , for reaction of  $W(CO)_5(CyH)$  with  $0.059\text{ mol L}^{-1}$  THF at  $T = 20^\circ\text{C}$ . The solid lines are single-exponential fits to the data with  $k_{\text{obs}} = 7.34 \times 10^5\text{ s}^{-1}$ .

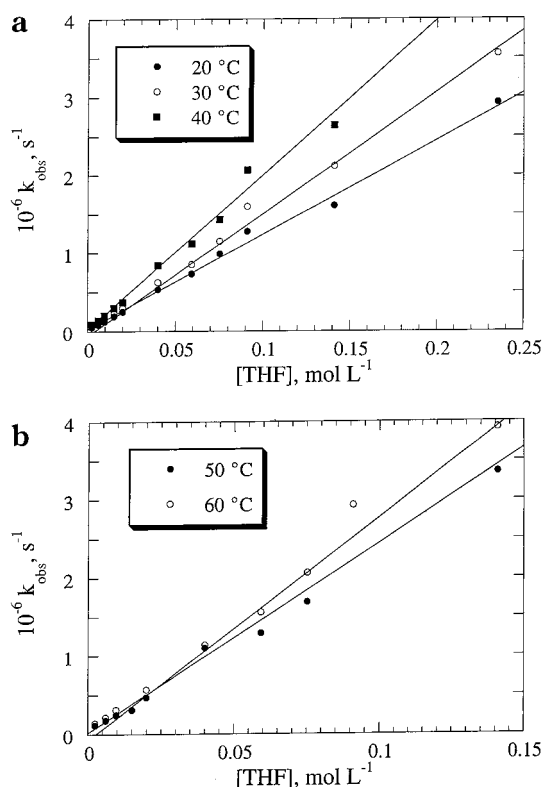


**Figure 4.** Experimental results for reaction of  $W(CO)_6-(CyH)$  with THF. The observed pseudo-first-order rate constant  $k_{\text{obs}}/10^6$  is plotted as a function of  $[THF]$ . Part a shows results for reaction at  $20^\circ\text{C}$  (●),  $30^\circ\text{C}$  (○), and  $40^\circ\text{C}$  (■); part b shows results for reaction at  $50^\circ\text{C}$  (●) and  $60^\circ\text{C}$  (○). The lines are linear fits to  $k_{\text{obs}}$  as a function of  $[THF]$ .

expense of the solvent, we hoped not to need a continuous flow of solution through the cell. To this end, we performed a preliminary experiment with CyH as the solvent in which successive kinetic runs were made with the solution flowing through the cell and then with no flow at all. We observed that the time dependence of the changes in the IR absorptions was independent of whether the solution was flowing through the cell and of the number of laser shots previously fired upon a particular sample. These observations imply that 308 nm photolysis of  $W(CO)_5(THF)$  regenerates the same intermediate produced by photolysis of  $W(CO)_6$ ; a

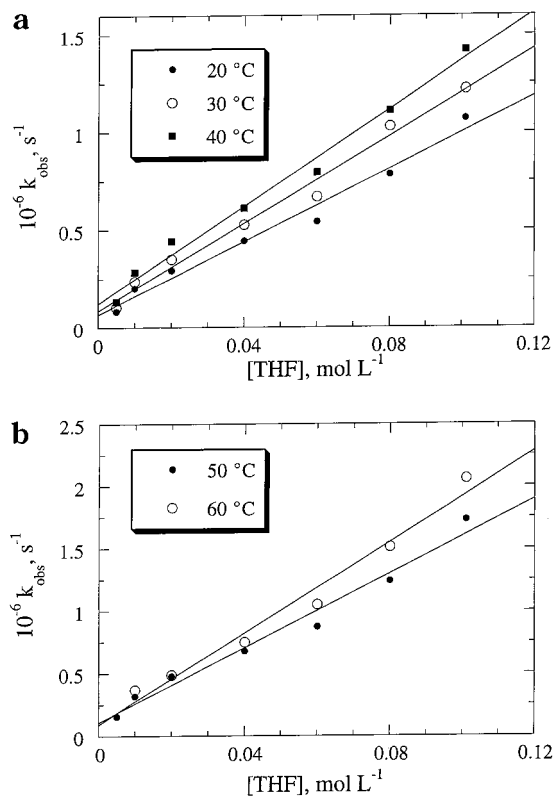


**Figure 5.** Experimental results for reaction of  $W(CO)_6-(CyD)$  with THF. The observed pseudo-first-order rate constant  $k_{\text{obs}}/10^6$  is plotted as a function of  $[THF]$ . Part a shows results for reaction at  $20^\circ\text{C}$  (●),  $30^\circ\text{C}$  (○), and  $40^\circ\text{C}$  (■); part b shows results for reaction at  $50^\circ\text{C}$  (●) and  $60^\circ\text{C}$  (○). The solid lines are linear fits to  $k_{\text{obs}}$  as a function of  $[THF]$ .

similar conclusion was reached by Dobson and co-workers regarding 351 nm photolysis of  $W(CO)_5(\text{hex-1-ene})$ .<sup>16</sup> Therefore, for the experiments in CyD, rather than flowing the solution through the cell into a "dump" flask, at each concentration of THF, a single solution was made, and that solution circulated through the cell. Furthermore, to minimize errors of measurement of small quantities of THF, for the experiments in CyD, a slightly different procedure was used for sample preparation. A stock solution of  $0.1\text{ M}$  THF in CyD was prepared, and aliquots of this solution were diluted to produce the solutions used in the various kinetic experiments. We also note that for reactions in CyD the majority of the reported rate constants were obtained from measurements of the rate of decay of the intermediate alone; each reported value of  $k_{\text{obs}}$  is the average of several independent kinetic runs.

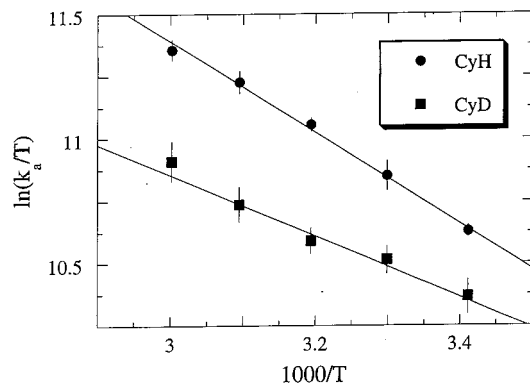
Results for  $k_{\text{obs}}$  as a function of  $[THF]$  are shown in Figure 5. Once again,  $k_{\text{obs}}$  is a linear function of  $[THF]$ , and the magnitudes of the pseudo-first-order rate constants are similar to, although somewhat smaller than, those observed in CyH.

## Discussion

**Activation Parameters and the Mechanism of Reaction 1.** Second-order rate constants " $k_a$ " are derived from the pseudo-first-order rate constants  $k_{\text{obs}}$  shown in Figures 4 and 5 at each temperature as the slopes of the linear fits to  $k_{\text{obs}}$  as a function of  $[THF]$  and are summarized in Table 1.

**Table 1. Second-Order Associative Rate Constants ( $k_a$ ) for Reaction 1 in CyH and CyD**

temperature, °C	$10^{-7} k_a(\text{CyH}), \text{L mol}^{-1} \text{s}^{-1}$	$10^{-7} k_a(\text{CyD}), \text{L mol}^{-1} \text{s}^{-1}$	$k_{\text{CyH}}/k_{\text{CyD}}$
20	$1.21 \pm 0.03$	$0.93 \pm 0.06$	$1.30 \pm 0.07$
30	$1.56 \pm 0.09$	$1.12 \pm 0.06$	$1.40 \pm 0.08$
40	$1.98 \pm 0.05$	$1.24 \pm 0.06$	$1.59 \pm 0.06$
50	$2.43 \pm 0.11$	$1.49 \pm 0.10$	$1.63 \pm 0.08$
60	$2.85 \pm 0.12$	$1.82 \pm 0.14$	$1.56 \pm 0.09$

**Figure 6.** Eyring analyses for reaction 1 in CyH (●) and CyD (■). The error bars are  $1\sigma$  uncertainties, and the solid lines are least-squares fits weighted by these uncertainties.

The linear fits shown in the figures have nonzero intercepts with values on the order of 1% of the values of the slopes. While the existence of these nonzero intercepts may indicate a small amount of dissociative (i.e., multistep reaction) behavior, we feel that a more likely interpretation is that in practice even at  $[\text{THF}] = 0$  the rate of disappearance of the intermediate will not be zero, due to reaction with unphotolyzed  $\text{W}(\text{CO})_6$ , recombination with CO, or reaction with impurities such as residual  $\text{H}_2\text{O}$ . The  $\text{W}(\text{CO})_5(\text{CyH})$  intermediate produced by photolysis of a solution of  $\text{W}(\text{CO})_6$  in CyH with no other reactant added has been observed to disappear with a rate constant of on the order of  $10^4 \text{ s}^{-1}$  (the exact reaction rate will obviously depend on the initial concentration of  $\text{W}(\text{CO})_6$  and the energy of the photolysis pulse).<sup>14</sup> Because the intercepts are so small relative to the slopes, they have not been further considered in our analyses.

From the temperature dependences of the second-order rate constants, we obtain Eyring activation parameters for reaction 1, Figure 6. For reaction of  $\text{W}(\text{CO})_5(\text{CyH})$ , we obtain  $\Delta H^\ddagger = 3.6 \pm 0.2 \text{ kcal mol}^{-1}$  and  $\Delta S^\ddagger = -13.7 \pm 3.5 \text{ eu}$ ; for reaction of  $\text{W}(\text{CO})_5(\text{CyD})$ , we obtain  $\Delta H^\ddagger = 2.4 \pm 0.6 \text{ kcal mol}^{-1}$  and  $\Delta S^\ddagger = -18.3 \pm 3.5 \text{ eu}$ .<sup>17</sup>

Evidence for the likely mechanism of reaction 1 can be obtained from the activation parameters. If reaction 1 were dissociative, we would expect the activation

enthalpy for the reaction as a whole to be at least  $10\text{--}15 \text{ kcal mol}^{-1}$ , since the reaction of “naked”  $\text{W}(\text{CO})_5$  should be nearly barrierless<sup>4</sup> and the  $\Delta H^\ddagger$  determined as described above should thus be near the  $(\text{CO})_5\text{W}$ –alkane bond dissociation energy (BDE), which generally are found to be of that order.<sup>3,18</sup> Thus, a much lower activation enthalpy ( $<5 \text{ kcal mol}^{-1}$ ) indicates the reaction is probably *not* dissociative. Furthermore, the strongly negative activation entropy indicates that the transition state for the reaction is significantly more ordered than the separated reactants, again evidence for an associative type of mechanism in which there is more bond forming than bond breaking at the transition state. This conclusion is also consistent with our  $\text{S}^2\text{FTIR}$  kinetics study<sup>19</sup> in which we discovered that the room-temperature reaction rate constant of reaction 1 varies directly with the ability of L to donate electrons as measured by the CO spectrum of the *product* complex. We explained this correlation in terms of the better ability of a strongly electron-donating ligand to stabilize an associative transition state by continuing to provide electron density at the nominally 16-electron metal center as the solvent molecule recedes.

To our knowledge, activation parameters for reaction 1 in CyH have only been reported three times previously. Dobson and Spradling<sup>20</sup> performed a TR-UV/vis study of reaction 1 with  $\text{L} = 4\text{-acetylpyridine}$  (4-acpy) and determined that  $\Delta H^\ddagger = 3.4 \pm 0.2 \text{ kcal mol}^{-1}$  and  $\Delta S^\ddagger = -13.0 \pm 0.6 \text{ eu}$ , and concluded from these results that the reaction proceeds by an associative mechanism. The close quantitative agreement between the activation parameters for THF and 4-acpy appears to be fortuitous, however.

In a second TR-UV/vis study, Dobson et al.<sup>16</sup> measured activation parameters for reaction 1 with  $\text{L} = \text{hex-1-ene}$ . The authors interpreted their results according to a purely dissociative mechanism, obtaining activation parameters for the solvent dissociation step of  $\Delta H_1^\ddagger = 8.2 \text{ kcal mol}^{-1}$  and  $\Delta S_1^\ddagger = -3.7 \text{ eu}$  and attributing the difference between  $\Delta H_1^\ddagger$  and the  $(\text{CO})_5\text{W}$ –CyH BDE to residual solvation of the “naked”  $\text{W}(\text{CO})_5$  intermediate. Careful reexamination of their raw data reveals, however, that their results are equally consistent with an *associative* mechanism for the reaction of  $\text{W}(\text{CO})_5(\text{CyH})$  with hex-1-ene, with  $\Delta H^\ddagger = 7.1 \text{ kcal mol}^{-1}$  and  $\Delta S^\ddagger = -8.0 \text{ eu}$ . Furthermore, Weiller<sup>21</sup> has deduced a dissociative mechanism for reaction 1 in liquid Xe ( $\text{L} = \text{CO}$ ) from his observation that  $\Delta H^\ddagger$  for reaction 1 in that system is the *same* to within experimental error as the gas-phase  $(\text{CO})_5\text{W}$ –Xe bond dissociation energy,<sup>22</sup> which is perhaps further evidence that the reaction of  $\text{W}(\text{CO})_5$ –(alkane) with hex-1-ene is associative after all.

A third study of reaction 1 in CyH was performed by Breheny et al.,<sup>23</sup> who investigated the recombination of several solvated group 6 intermediates including  $\text{W}(\text{CO})_5$ –(CyH) with CO. They reported that for this reaction  $\Delta H^\ddagger$

(18) Burkey, T. J. Personal communication.

(19) Schultz, R. H.; Krav-Ami, S. *J. Chem. Soc., Dalton Trans.* **1999**, 115.(20) Dobson, G. R.; Spradling, M. D. *Inorg. Chem.* **1990**, *29*, 880.(21) (a) Weiller, B. H. *J. Am. Chem. Soc.* **1992**, *114*, 10910. (b) Weiller, B. H.; Wasserman, E. P.; Moore, C. B.; Bergman, R. G. *J. Am. Chem. Soc.* **1993**, *115*, 4326.(22) Wells, J. R.; Weitz, E. *J. Am. Chem. Soc.* **1992**, *114*, 2783.(23) Breheny, C. J.; Kelly, J. M.; Long, C.; O’Keeffe, S.; Pryce, M. T.; Russell, G.; Walsh, M. M. *Organometallics* **1998**, *17*, 3690.

(17) These second-order rate constants “ $k_a$ ” assume an associative, single-step mechanism. A reviewer has pointed out that our kinetic results are also consistent with simultaneous associative and dissociative reaction. In fact, under our experimental conditions, it is possible that even a purely dissociative reaction would be kinetically indistinguishable from a purely associative reaction (Lugovskoy, S.; Schultz, R. H. Work in progress)! For a dissociative mechanism in which the W–alkane bond is broken before the THF molecule arrives, the reported  $\Delta H^\ddagger$  will be  $\Delta H_1^\ddagger - \Delta H_2^\ddagger + \Delta H_3^\ddagger$ , where  $\Delta H_1^\ddagger$  and  $\Delta H_2^\ddagger$  refer to the dissociation and formation of  $(\text{CO})_5\text{W}$ –alkane and  $\Delta H_3^\ddagger$  refers to the formation of the product. As discussed below, we feel that a dissociative mechanism is extremely unlikely for this reaction, but it cannot be ruled out on kinetic grounds alone.

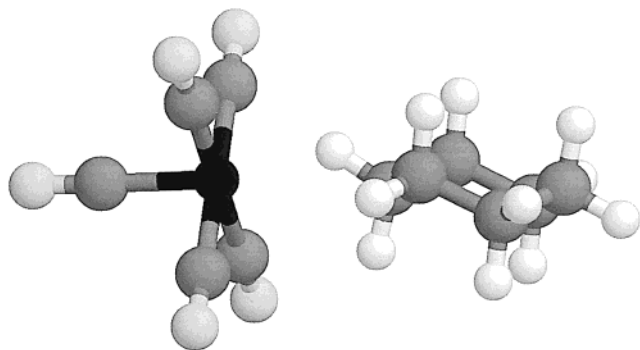


**Figure 7.** Equilibrium structure of  $W(CO)_5(CyH)$  as calculated by DFT.

$= 5.5 \text{ kcal mol}^{-1}$  and  $\Delta S^\ddagger = -14 \text{ eu}$ . While it might seem surprising that the enthalpy of activation for reaction with CO is higher than that for reaction with THF, these results are in fact consistent with an associative mechanism in which reaction of an electron-withdrawing ligand will tend to have a higher  $\Delta H^\ddagger$  than reaction of an electron-donating one.

In the strictest sense, however, an “associative” ligand exchange reaction (type A in the Langford-Gray notation<sup>24</sup>) requires detection of an intermediate of increased coordination number. We have not detected such an intermediate in our studies, and to our knowledge, “ $W(CO)_5(solv)(L)$ ” has never been detected as a species with an independent existence. In the context of the experimental results presented here and in our previous paper, it seems most reasonable to consider reaction 1 with  $L = \text{THF}$  as occurring via an “associative interchange” ( $I_a$ ) process.

**Ab Initio Calculation of  $W(CO)_5(CyH)$ .** To our knowledge, except for measurements of IR C–O stretching frequencies and of UV/vis spectra, no  $W(CO)_5$ -(alkane) complex has been characterized experimentally, and the only theoretical characterization of such complexes has been an ab initio MP2 calculation of  $W(CO)_5$  complexation with small ( $C_1$ – $C_3$ ) alkanes and fluoroalkanes performed by Zarić and Hall.<sup>25</sup> To better understand the dynamics of reaction 1 and the observed isotope effect in the present system, we therefore performed an ab initio DFT calculation<sup>26</sup> at the B3LYP/CEP-31G\* level with full optimization in order to determine the equilibrium structure and vibrational frequencies for  $W(CO)_5(CyH)$  and  $W(CO)_5(CyD)$ . The optimized geometry for the  $W(CO)_5(CyH)$  complex is shown pictorially in Figure 7, and some geometrical parameters of interest are given in Table 2.

We find that in the complex the W atom does not sit symmetrically relative to the nearest methylene of the

**Table 2.** Geometrical Parameters for  $W(CO)_5(CyH)$  As Determined by DFT

atom pair <sup>a</sup>	bond length, Å	atoms ABC <sup>a</sup>	$\angle ABC$ , deg
W–C <sup>α</sup>	2.998	C <sup>cis</sup> –W–C <sup>cis</sup>	179.9
W–H <sup>α1</sup>	2.116	C <sup>trans</sup> –W–C <sup>cis</sup>	89.9
W–H <sup>α2</sup>	2.993	O–C–W	179.0
W–C <sup>cis</sup>	2.065	W–H <sup>α1</sup> –C <sup>α</sup>	132.2
W–C <sup>trans</sup>	1.978	W–H <sup>α2</sup> –C <sup>α</sup>	79.6
C <sup>cis</sup> –O	3.231	C <sup>trans</sup> –W–H <sup>α1</sup>	168.8
C <sup>trans</sup> –O	3.152	C <sup>trans</sup> –W–H <sup>α2</sup>	153.8
C <sup>α</sup> –H <sup>α1</sup>	1.135	H <sup>α1</sup> –C <sup>α</sup> –H <sup>α2</sup>	110.7
C <sup>α</sup> –H <sup>α2</sup>	1.101	H–C–H (av)	106.9
C–H (av)	1.105		
C–C (av)	1.551		

<sup>a</sup> C<sup>cis</sup> = carbonyl C cis to CyH; C<sup>trans</sup> = carbonyl C trans to CyH; C<sup>α</sup> = CyH C nearest to W.

CyH molecule. Rather, the  $W(CO)_5$  fragment interacts primarily with a single equatorial C–H bond of CyH in a manner qualitatively similar to the optimized geometries that Zarić and Hall<sup>25</sup> found for the complexes with the smaller alkanes. This C–H bond lengthens slightly, from 1.10 to 1.14 Å (for smaller alkanes, Zarić and Hall calculated that this bond lengthens to about 1.16 Å). The CyH ring lies at an angle of approximately 45° relative to adjacent cis carbonyls. As expected for such a weakly bound complex, the geometry of the  $W(CO)_5$  fragment is essentially unchanged from its geometry in  $W(CO)_6$ ,<sup>27</sup> except that the W–C bond trans to the CyH molecule contracts by approximately 0.1 Å. Bond lengths and angles of the other bonds of CyH are not significantly altered from their values in the free molecule.

To obtain more accurate estimates of the vibrational spectra of the complexes, we also performed a calculation at the same level of theory on the CyH and CyD molecules. We found that the calculated vibrational frequencies of CyH and CyD required a scaling factor of  $\sim 0.94$  in order to match the experimental values;<sup>28</sup> the use of such a correction factor is typical for ab initio calculations of vibrational structure.<sup>29</sup> By using the scaling factor determined from CyH and CyD for the calculated vibrational frequencies of the  $W(CO)_5(CyH)$  and  $W(CO)_5(CyD)$  complexes, we were able to reproduce the experimentally observed C–O stretching frequencies to within 1%. Representative vibrational frequencies of interest are given in Table 3.

Of the 81 vibrational modes of  $W(CO)_5(C_6H_{12})$ , 48 can be attributed to the  $C_6H_{12}$  molecule, 27 to the  $W(CO)_5$  fragment, and the remaining 6 to the  $(CO)_5W$ – $C_6H_{12}$  stretch, the two  $(CO)_5W$ – $C_6H_{12}$  bends, and the three hindered rotations of the  $C_6H_{12}$  molecule. In Table 3, we list frequencies for those modes that contain the largest components of the two  $(CO)_5W$ – $C_6H_{12}$  bending motions and of the three hindered rotations, but it should be noted that many low-frequency modes nominally of the  $W(CO)_5$  skeleton alone also show a dependence on the  $C_6H_{12}$  isotopomer present in the complex. Since motions of the CyH ring are necessary to com-

(24) Langford, C. H.; Gray, H. B. *Ligand Substitution Processes*; W. A. Benjamin: New York, 1966.

(25) Zarić, S.; Hall, M. B. *J. Phys. Chem. A* **1997**, *101*, 4646.

(26) Frisch, M. J.; Trucks, G. W.; Schlegel, H. B.; Scuseria, G. E.; Robb, M. A.; Cheeseman, J. R.; Zakrzewski, V. G.; Montgomery, J. A.; Stratmann, R. E.; Burant, J. C.; Dapprich, S.; Millam, J. M.; Daniels, A. D.; Kudin, K. N.; Strain, M. C.; Farkas, O.; Tomasi, J.; Barone, V.; Cossi, M.; Cammi, R.; Mennucci, B.; Pomelli, C.; Adamo, C.; Clifford, S.; Ochterski, J.; Petersson, G. A.; Ayala, P. Y.; Cui, Q.; Morokuma, K.; Malick, D. K.; Rabuck, A. D.; Raghavachari, K.; Foresman, J. B.; Cioslowski, J.; Ortiz, J. V.; Stefanov, B. B.; Liu, G.; Liashenko, A.; Piskorz, P.; Komaromi, I.; Gomperts, R.; Martin, R. L.; Fox, D. J.; Keith, T.; Al-Laham, M. A.; Peng, C. Y.; Nanayakkara, A.; Gonzalez, C.; Challacombe, M.; Gill, P. M. W.; Johnson, B. G.; Chen, W.; Wong, M. W.; Andres, J. L.; Head-Gordon, M.; Replogle, E. S.; Pople, J. A. *Gaussian 98* (Revision A.7); Gaussian, Inc.: Pittsburgh, 1998.

(27) Arnesen, S. P.; Seip, H. M. *Acta Chem. Scand.* **1966**, *20*, 2711.

(28) (a) Shimanouchi, T. *Tables of Molecular Vibrational Frequencies, Consolidated Volume I*; National Bureau of Standards: Washington, D.C., 1972. (b) Sverdlov, L. M.; Kovner, M. A.; Krainov, E. P. *Vibrational Spectra of Polyatomic Molecules*; translated from the Russian by the IPST staff; Wiley: New York, 1973. (c) Dorofeeva, O. V.; Gurvich, L. V.; Jorish, V. S. *J. Phys. Chem. Ref. Data* **1986**, *15*, 437.

(29) Hehre, W. J.; Radom, L.; Schleyer, P. v. R.; Pople, J. A. *Ab Initio Molecular Orbital Theory*; Wiley: New York, 1986; Chapter 6.



**Table 3. Selected Calculated<sup>a</sup> Vibrational Frequencies (cm<sup>-1</sup>) for W(CO)<sub>5</sub>(CyH) and W(CO)<sub>5</sub>(CyD)**

vibration	W(CO) <sub>5</sub> (CyH)	W(CO) <sub>5</sub> (CyD)
W–CyH (CyD) hindered rotation <sup>b</sup>	73, 116, 144	71, 114, 127
W–CyH (CyD) bend <sup>b</sup>	55, 84	58, 82
W–CyH (CyD) stretch	124	122
C–O stretch	1933, 1949, 1977, 2061 <sup>c</sup>	1936, 1949, 1977, 2061
C <sup>α</sup> –H <sup>α</sup> stretch	2578	1893
C–H stretch	2892, 2893, 2894, 2898, 2901, 2935, 2937, 2938, 2946, 2948, 2962	2119, 2120, 2124, 2125, 2130, 2181, 2188, 2190, 2197, 2200, 2207

<sup>a</sup> Corrected values; see text. <sup>b</sup> Contain some amount of W(CO)<sub>5</sub> skeletal motion; see text. <sup>c</sup> Experimental values for the three IR-active vibrations are 1928, 1954, and 2087 cm<sup>-1</sup>.

compensate for any motion of the W(CO)<sub>5</sub> in order to maintain the center of mass, there will necessarily be mixing of “W–C<sub>6</sub>H<sub>12</sub> bending” into the low-frequency carbonyl modes, and CyH “bending” and “hindered rotational” motions are actually combinations of low-frequency carbonyl bends with bending of the CyH ring against the W(CO)<sub>5</sub> skeleton.

We calculate that a C–H (C–D) stretching vibration associated with the H(D) atom closest to the W atom drops in frequency by some 10% relative to its frequency in the free alkane. Except for the lowering of this frequency and loss of degeneracy of the E<sub>g</sub> and E<sub>u</sub> vibrational modes of the free alkane due to the lowering of symmetry, the remaining vibrational frequencies associated with motions of the CyH molecule itself do not alter very much upon complexation. We also obtain a (CO)<sub>5</sub>W–CyH bond dissociation enthalpy (after correction to 298 K) of  $\Delta H = 13.6$  kcal/mol, which is in good (although arguably fortuitous<sup>30</sup>) agreement with the experimental gas-phase value of  $11.6 \pm 3$  kcal/mol.<sup>31</sup> The specific applications of the results of our calculation to our experimental results will be discussed in the succeeding sections.

**Solvent Isotope Effects on  $\Delta S^\ddagger$  in Reaction 1.** As shown in Figures 4–6 and Table 1, at all temperatures studied, reaction 1 shows a “normal” kinetic isotope effect in which the second-order rate constant is larger in CyH than in CyD. The *relative* rate of reaction in the two solvents appears to be temperature-dependent, however. Since the second-order rate constant is a more quickly rising function of temperature in CyH than in CyD, it appears that the enthalpy of activation must be higher in CyH even though  $k_{\text{obs}}$  itself is higher in CyH at all temperatures measured. The Eyring analysis presented in Figure 6 indicates that  $\Delta H^\ddagger$  is indeed lower in CyD and that the differences in second-order rate constants are due primarily to *entropic* effects.

As we saw above,  $\Delta S^\ddagger$  of reaction 1 is negative, indicating an overall loss of the number of degrees of freedom as the reaction system approaches the transition state, consistent with the late transition state of

an associative reaction. Since  $\Delta H^\ddagger$  is lower in CyD than in CyH, yet the reaction rate constant is lower,  $\Delta S^\ddagger$  must be more negative in CyD than in CyH ( $\Delta\Delta S^\ddagger = 4.6 \pm 4.3$  eu). A plausible explanation for this difference relies on the effect of low-frequency bending and hindered rotational motions on the overall entropy of the complex. Since these motions are of lower frequency in the CyD complex than in the CyH complex (Table 2), they will be more highly populated in the former. As the system approaches the transition state, these degrees of freedom will be lost as the solvent molecule leaves, causing  $\Delta S^\ddagger$  to be more negative when the reaction takes place in CyD.<sup>32</sup>

Similar considerations have been invoked in other studies of isotope effects in  $\sigma$ -binding of C–H(D) bonds to transition metal centers. While Calvert and Shapley<sup>33</sup> reported that in the compound  $\text{HOS}_3(\text{CO})_{10}\text{CH}_n\text{D}_{3-n}$  the agostic Os–H(D)–C interaction favors Os–H over Os–D binding, due to zero-point energy (ZPE) effects that will preferentially weaken a C–H bond relative to a C–D bond, theoretical studies indicate that low-frequency vibrations and hindered rotations of a  $\sigma$ -bound molecule not involving the three-center bond itself can contribute significantly to the overall energy of the complex, leading to an inverse EIE in the binding of a small molecule to a TM center.<sup>11,12</sup> Similarly, Parkin and co-workers<sup>34</sup> have explained the inverse EIE observed in H<sub>2</sub> or D<sub>2</sub> addition to  $\text{M}(\text{PMe}_3)_4\text{X}_2$  (M = Mo or W, X = halide) in terms of contributions of isotope-sensitive vibrational frequencies other than that of the M–H(D) stretch.

Two experimental studies of isotope effects in reactions of metal–alkane complexes have been performed previously. Zhang and Dobson<sup>35</sup> observed that at room temperature ligand substitution by hex-1-ene at  $\text{Cr}(\text{CO})_5(\text{solv})$  is faster for  $\text{solv} = \text{octane-}d_0$  than it is for  $\text{solv} = \text{octane-}d_{18}$ . They reported a ratio  $k_{\text{H}}/k_{\text{D}} = 1.4$  in the room-temperature reaction rate constants, similar in magnitude to that observed in the present study with L = THF and  $\text{solv} = \text{CyH}$  or  $\text{CyD}$ . They explained this “normal” isotope effect as being due to more bond breaking than bond forming in the transition state, since an M–D bond is expected to have a lower ZPE than an M–H bond. Our observation of  $\Delta S^\ddagger < 0$  for reaction in CyD calls this interpretation into question, however.

As mentioned in the Introduction, Bergman and Moore and co-workers investigated the alkane C–H bond activation reactions of photolytically produced  $\text{Cp}^*\text{Rh}(\text{CO})(\text{Kr})$  with CyH and neopentane and their deuteriated analogues in liquid Kr solution.<sup>9</sup> Although they could not measure the properties of the  $\text{Cp}^*\text{Rh}(\text{CO})$ –alkane complex directly, their kinetic re-

(32) An alternative explanation for the differences in activation parameters for reaction in the two solvents has been suggested to us, according to which the “bulkier” CyH molecule must move further away from the metal center than CyD in order to give the THF molecule access to the metal center. While we cannot absolutely rule out this explanation, we feel that it is unlikely, as the bond lengths of CyH and CyD are virtually identical, and the mean vibrational amplitudes differ by an amount only on the order of 1% of the size of the molecule (Ewbank, J. D.; Kirsch, G.; Schaefer, L. *J. Mol. Struct.* **1976**, *31*, 39).

(33) Calvert, R. B.; Shapley, J. R. *J. Am. Chem. Soc.* **1978**, *100*, 7726.

(34) (a) Rabinovitch, D.; Parkin, G. *J. Am. Chem. Soc.* **1993**, *115*, 353. (b) Hascall, T.; Rabinovitch, D.; Murphy, V. J.; Beachy, M. D.; Friesner, R. A.; Parkin, G. *J. Am. Chem. Soc.* **1999**, *121*, 11402.

(35) Dobson, G. R.; Zhang, S. Unpublished results cited in: Zhang, S.; Dobson, G. R.; Zang, V.; Bajaj, H. C.; van Eldik, R. *Inorg. Chem.* **1990**, *29*, 9, 3477.

(30) Zarić and Hall<sup>25</sup> reported that their calculated dissociation energies for (CO)<sub>5</sub>W–alkane complexes did not converge monotonically at increasingly high levels of theory, but rather oscillated around the true value.

(31) Brown, C. E.; Ishikawa, Y.-I.; Hackett, P. A.; Rayner, D. M. *J. Am. Chem. Soc.* **1990**, *112*, 2530.

sults strongly implied an inverse EIE for the binding of an alkane to  $Cp^*Rh(CO)$  and that, moreover, this EIE is driven almost entirely by differences in  $\Delta S^\ddagger$  (much as is observed here for binding to  $W(CO)_5$ ). They attributed this entropic effect to differences in the populations of low-frequency vibrational and hindered rotational modes. While Breheny et al.<sup>23</sup> did not measure isotope effects, they reached a similar conclusion from their observation of a dependence of  $\Delta S^\ddagger$  on the solvent size for recombination of a given TM fragment with CO in a series of alkane solvents.

Thus, we can see that the inverse isotope effect on  $\Delta S^\ddagger$  observed in reaction 1 is not unreasonable. In the present case (and presumably in that of Zhang and Dobson<sup>35</sup> as well), however, the inverse isotope in the entropy of activation is insufficient to overcome the difference in the enthalpic barrier, and the overall kinetic isotope effect (KIE) is normal.

#### Solvent Isotope Effects on $\Delta H^\ddagger$ in Reaction 1.

Next, we consider the effect of solvent deuteration on the activation enthalpy of reaction 1. We observe that  $\Delta H^\ddagger$  is significantly lower in CyD even though the reaction proceeds more slowly. In this section, we discuss qualitatively what effects might lead to a lower activation enthalpy in CyD than in CyH. Inverse KIEs have been seen previously<sup>36</sup> in reductive elimination reactions of  $X-M-H$  complexes in which a metal-hydrogen bond is broken and a new bond with a higher  $X-H$  stretching frequency is formed. In these reactions, an inverse KIE is seen because the reaction has a late transition state in which the  $C-H$  bond is already fully formed or nearly so. In such a case, the ZPE change will be less for  $C-D$  bond formation than for  $C-H$  bond formation, so the activation enthalpy will be lower for the deuteriated complex.

While in the present experiments, the  $C-H(D)$  bond of the alkane is not broken, it is reasonable to assume that similar effects are influencing the course of reaction 1. For an  $I_a$  reaction 1, the  $W-solv$   $\sigma$ -interaction will be greatly diminished at the transition state relative to that of the  $W(CO)_5(solv)$  complex. Just as with reductive elimination, the "formation" (or, perhaps more accurately, reconstruction) of a stronger bond engenders a smaller ZPE change and therefore a lower enthalpic barrier to reaction in CyD. Indeed, when we use the vibrational frequencies obtained from our ab initio calculation to calculate the relative ZPE change upon dissociation of the  $W(CO)_5(alkane)$  complex into  $W(CO)_5 + CyH$  or  $CyD$ , we find that the overall ZPE change is approximately  $20\text{ cm}^{-1}$  less for dissociation of the  $CyD$  complex than for the  $CyH$  complex.

It thus appears that the "normal" KIE observed in reaction 1 is in fact due to a combination of two "inverse" isotope effects. The additional vibrational density of states available to the  $W(CO)_5(CyD)$  complex means that reaction 1 has a more negative  $\Delta S^\ddagger$  in  $W(CO)_5(CyD)$  than in  $W(CO)_5(CyH)$ . On the other hand, the late transition state typical of an associative reaction leads to a lower  $\Delta H^\ddagger$  for loss of  $CyD$ . In the case of reaction 1, the entropic effect is more significant, so  $\Delta G^\ddagger$  is higher for reaction in  $CyD$ , and we see a "normal" isotope effect;

that is, reaction proceeds more rapidly in  $CyH$  in the temperature range studied here.

**Reaction 1 and Statistical Mechanical Models for Isotope Effects.** In the past few years, a number of workers have considered isotope effects in reactions of organometallic species in terms of equilibrium statistical mechanics.<sup>5,12,37</sup> The equilibrium constant ( $K_{eq}$ ) for reaction 2,

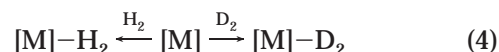


where asterisks indicate isotopically labeled species, is given by eq 3,

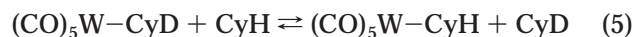
$$K_{eq} = \left( \frac{Q_{tr}^{A^*} Q_{rot}^{A^*} Q_{vib}^{A^*}}{Q_{tr}^A Q_{rot}^A Q_{vib}^A} \right) \left( \frac{Q_{tr}^B Q_{rot}^B Q_{vib}^B}{Q_{tr}^{B^*} Q_{rot}^{B^*} Q_{vib}^{B^*}} \right) e^{-\Delta\Delta ZPE/RT} \quad (3)$$

where  $Q_{tr}$ ,  $Q_{rot}$ , and  $Q_{vib}$  are the translational, rotational, and vibrational partition functions of the various species, and  $\Delta\Delta ZPE$  is the overall change in ZPE, i.e.,  $(ZPE^{B^*} + ZPE^A) - (ZPE^B + ZPE^{A^*})$ . The expression on the right side of eq 3 is normally written as the product of four terms: SYM, a "symmetry" term arising from the rotational partition functions; MMI, a "mass and moment of inertia" term from the translational and rotational partition functions; EXC, an "excitation" term arising from population of excited vibrational states reflected in the vibrational partition functions; and ZPE, the exponential that includes the zero-point energies.

This model has been used successfully to explain EIEs in the binding of dihydrogen<sup>38</sup> and ethylene<sup>11</sup> to transition-metal complexes and isotope effects in oxidative addition of  $H-H$  ( $D-D$ ) and  $C-H$  ( $C-D$ ) bonds<sup>12,34</sup> of the type shown as reaction 4:



To gain a better understanding of the dynamics of reaction 1 and to support the conclusions described above, we used the results of the ab initio calculation of the structure of  $W(CO)_5(CyH)$  in order to model the EIE for the exchange of  $CyD$  and  $CyH$  at the  $W(CO)_5$  center, reaction 5; note that for this reaction the SYM terms cancel.



For reaction 5, the two terms in eq 3 that are related to the vibrational partition function, EXC and ZPE, both favor formation of  $(CO)_5W-CyD$  (i.e., predict an inverse EIE): we find that at 298 K, EXC = 0.924 and ZPE = 0.918.<sup>39</sup> That is, as discussed above, the additional low-

(36) (a) Jones, W. D.; Feher, F. J. *Acc. Chem. Res.* **1989**, *22*, 91. (b) Rosini, G. P.; Soubra, S.; Vixamar, M.; Wang, S.; Goldman, A. S. *J. Organomet. Chem.* **1998**, *554*, 41.

(37) (a) Bigeleisen, J.; Goeppert-Mayer, M. *J. Chem. Phys.* **1947**, *15*, 261. (b) McLennan, D. J. *Isotopes in Organic Chemistry*; Buncl, E., Lee, E., Eds.; Elsevier: New York, 1987; Vol. 7, Chapter 6, pp 393–480.

(38) Bender, B. R.; Kubas, G. J.; Jones, L. H.; Swanson, B. I.; Eckert, J.; Capps, K. B.; Hoff, C. D. *J. Am. Chem. Soc.* **1997**, *119*, 9179.

(39) While only "isotope-sensitive modes" will contribute to the overall isotope effect, as discussed above, many nominally insensitive modes do have some isotope dependence. Therefore, we calculated the complete partition functions using the calculated geometries and corrected vibrational frequencies for all four species. Values for fundamental constants were taken from: Cohen, E. R.; Taylor, B. N. *Phys. Today* **1999**, *52*, BG5.



frequency vibrational modes available to the CyD complex cause its formation to be slightly favored.<sup>40</sup>

For the MMI term, we calculate  $\text{MMI} = 1.541$ , i.e., tending toward a normal isotope effect; a similar tendency was reported by Bender<sup>11</sup> for complexation of  $\text{C}_2\text{H}_4$  and  $\text{C}_2\text{D}_4$  to  $\text{Os}_2(\text{CO})_8$ . The normal isotope effect for the MMI term arises because the ratios of the masses and of  $I_A I_B I_C$  (product of the moments of inertia) are larger for the CyD/CyH pair than for the  $\text{W}(\text{CO})_5(\text{CyD})/\text{W}(\text{CO})_5(\text{CyH})$  pair. Thus, the additional translational and rotational degrees of freedom available to the  $\text{W}(\text{CO})_5(\text{CyD})$  complex relative to  $\text{W}(\text{CO})_5(\text{CyH})$  do not make up for the degrees of freedom lost by the CyD molecule upon complexation. It is not clear, however, if the MMI term calculated from the partition functions accurately reflects the true situation for reaction 5 in solution. The MMI term reported above is calculated from the complete rotational and translational partition functions and thus assumes unhindered rotation and translation for all of the species involved in the equilibrium. While such assumptions are probably good for H and D<sub>2</sub>,<sup>41</sup> the rotation of CyH in liquid cyclohexane itself is somewhat hindered;<sup>42</sup> clearly, the assumption of free rotation and translation for the complex is almost certainly not justified. We also note that use of the Teller–Redlich product rule,<sup>11,34,38,43</sup> which relates the translational and rotational partition functions to the molecular vibrations, yields  $\text{MMI} = 1.199$ , in reasonable agreement with the MMI calculated directly from  $Q_{\text{tr}}$  and  $Q_{\text{rot}}$ .

The three factors ( $\text{EXC} \times \text{ZPE} \times \text{MMI}$ ) calculated from the partition functions combine to predict a normal overall EIE for reaction 5 of 1.30. If we use the MMI predicted from the Teller–Redlich product rule, we obtain an EIE of 1.01. In the limit that  $\text{MMI} = 1$  (i.e., rotational and translational densities of states are identical for the two sides of reaction 5), we obtain an *inverse* overall EIE of 0.846. Thus, while we cannot say absolutely which side of reaction 5 is favored, it is clear that the *vibrational* degrees of freedom favor formation of  $\text{W}(\text{CO})_5(\text{CyD})$  and that it is the loss of these degrees of freedom at the transition state that causes  $\Delta S^\ddagger$  to be more negative for reaction of  $\text{W}(\text{CO})_5(\text{CyD})$  than for  $\text{W}(\text{CO})_5(\text{CyH})$ . In any event,  $\Delta G$  for reaction 5 is  $<0.2$  kcal/mol, indicating that  $\Delta\Delta G^\circ$  for the two complexes is essentially the inverse of the  $\Delta\Delta G^\circ$  for CyH and CyD,  $\sim 1.7$  kcal/mol;<sup>44</sup> the uncertainties in the free energies of formation of  $\text{C}_6\text{H}_{12}$  and  $\text{C}_6\text{D}_{12}$  and of  $\Delta G^\ddagger$  for reaction 1 are larger than the  $\Delta G$  of reaction 5. The calculation of the EIE for reaction 5 enables us to construct the free

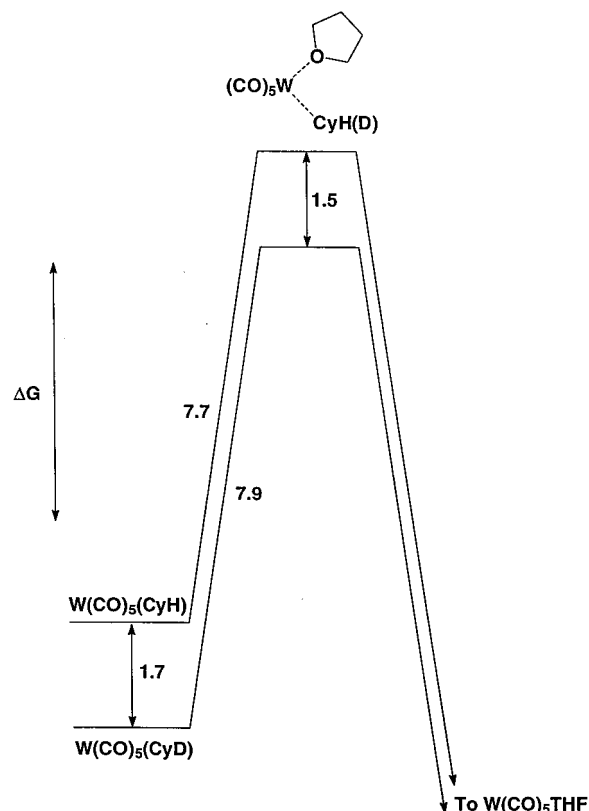


**Figure 8.** Free energy diagram for the reaction of  $\text{W}(\text{CO})_5(\text{CyH})$  and  $\text{W}(\text{CO})_5(\text{CyD})$  with THF. The ordinate is  $\Delta G$  in kcal/mol at 298 K for reaction 1 for the two complexes.  $\Delta\Delta G^\circ$  for the starting complexes was derived from the DFT calculation as described in the text, and  $\Delta G^\ddagger$  from the experimental results.

energy diagram for reaction 1 shown in Figure 8, which makes it clear that even though  $\Delta H^\ddagger$  is lower for  $\text{W}(\text{CO})_5(\text{CyD})$  than it is for  $\text{W}(\text{CO})_5(\text{CyH})$ , the overall KIE is normal; that is,  $\Delta\Delta G$  at the transition state is smaller than it is in the ground state.

## Conclusions

In this study, we use TRIR spectroscopy to measure the kinetics and thermodynamics of the ligand reaction of  $\text{W}(\text{CO})_5(\text{solv})$  with THF for  $\text{solv} = \text{cyclohexane (CyH)}$  and  $\text{cyclohexane-}d_{12} \text{ (CyD)}$ . We have determined the activation parameters for this reaction to be  $\Delta H^\ddagger = 3.6 \pm 0.2$  kcal mol<sup>-1</sup>,  $\Delta S^\ddagger = -13.7 \pm 2.5$  eu for  $\text{solv} = \text{CyH}$ , and  $\Delta H^\ddagger = 2.4 \pm 0.6$  kcal mol<sup>-1</sup>,  $\Delta S^\ddagger = -18.3 \pm 3.5$  eu for  $\text{solv} = \text{CyD}$ . The low enthalpies of activation and negative entropies of activation indicate that the reaction proceeds through an associative interchange ( $I_a$ ) mechanism. In addition, the observed isotope effects are consistent with an  $I_a$  mechanism as well. “Freezing out” of low-frequency vibrational modes at the transition state leads to a more negative  $\Delta S^\ddagger$ , while the breakdown of the  $\text{M}-(\text{C}-\text{H})$   $\sigma$ -interaction at the transition state leads to a lower  $\Delta H^\ddagger$  for reaction in CyD. Over the temperature range studied here, the overall  $\Delta G^\ddagger$  is higher in CyD, leading to a “normal” kinetic isotope effect. Finally, an *ab initio* calculation of the structures and vibrational spectra of  $\text{W}(\text{CO})_5(\text{C}_6\text{H}_{12})$  and  $\text{W}(\text{CO})_5(\text{C}_6\text{D}_{12})$  reveals that the tungsten atom interacts with the alkane primarily through a single C–H bond and

(40) Bergman and co-workers<sup>9</sup> reported that for  $\text{Rh}(\text{CO})_2$  at 165 K formation of the CyD complex is favored over formation of the CyH complex by a factor of approximately 10. Our calculations indicate that for  $\text{W}(\text{CO})_5$  the equilibrium does move more toward the CyD complex, but by a considerably more modest amount (about 5% difference between 298 and 165 K).

(41) (a) Taylor, D. G., III; Strauss, H. L. *J. Chem. Phys.* **1989**, *90*, 768. (b) Hunter, J. E., III; Taylor, D. G. III; Strauss, H. L. *J. Chem. Phys.* **1992**, *97*, 50.

(42) (a) Farman, H.; Dore, J. C.; Bellissent-Funel, M.-C. *Mol. Phys.* **1987**, *61*, 583. (b) Farman, H.; O'Mard, L.; Dore, J. C.; Bellissent-Funel, M.-C. *Mol. Phys.* **1991**, *73*, 855.

(43) McQuarrie, D. A. *Statistical Mechanics*; Harper & Row: New York, 1976; p 148.

(44) Calculated from  $\Delta H^\circ$  and  $\Delta S^\circ$  data cited in: Afeefy, H. Y.; Liebman, J. R.; Stein, S. E. *Neutral Thermochemical Data*. In *NIST Chemistry Webbook, NIST Standard Reference Database Number 69*; Mallard, W. G., Lindstrom, P. J., Eds.; National Institutes of Standards and Technology: Gaithersburg, MD, 1998 (<http://webbook.nist.gov>).

that the proposed explanation for the observed kinetic isotope effect in the reaction of the complex with THF is consistent with the structures and vibrational spectra obtained from the *ab initio* calculation.

**Acknowledgment.** This research was supported in part by a grant from the Israel Foundation, administered by the Israel Academy of Arts and Sciences; by the U.S.-Israel Binational Science Foundation; and by the Bar-Ilan University Research Authority. In addition, partial funding for the diode laser spectrometer was provided by the Rashi Foundation as part of a Guastalla Fellowship awarded to R.H.S. from 1994 to 1997. The *ab initio* calculations were performed by Dr. Pinchas

Aped of the Bar-Ilan Department of Chemistry. The technical assistance of the members of the Bar-Ilan University Electronics Shop is also gratefully acknowledged. Finally, R.H.S. would like to acknowledge Dr. H. Schultz for bringing ref 15a to his attention and for useful discussions regarding the statistical analyses.

**Supporting Information Available:** Tables of experimentally obtained pseudo-first-order reaction rate constants, calculated atomic coordinates for  $W(CO)_5(CyH)$ , and calculated vibrational frequencies for  $W(CO)_5(CyH)$  and  $W(CO)_5(CyD)$ . This material is available free of charge via the Internet at <http://pubs.acs.org>.

OM990828Y